

Lipogels: Single Lipid Bilayer-Enclosed Hydrogel Spheres

Qasim Saleem,^{1,2} Baoxu Liu,^{2,3} Claudiu C. Gradinaru,^{2,3}
and Peter M. Macdonald^{1,2}

Department of Chemistry¹ and Department of Physics³
University of Toronto

and

Department of Chemical and Physical Sciences²
University of Toronto Mississauga
3359 Mississauga Road North
Mississauga, Ontario, Canada L5L 1C6

SUPPORTING INFORMATION:

NMR Spectra and Analysis:

NMR spectra were acquired by the methods listed in the main paper. Due to well separated tetradecylamine and NIPAM resonances, the ¹³C NMR spectrum (Figure S1) was used to assess AA modification. Essentially, since the AAs were modified by tetradecylamine, the mole ratio of AA to NIPAM (pre-modification) could be compared to the mole ratio of tetradecylamine to NIPAM (post-modification) to determine the extent of modification. To determine the AA to NIPAM mole ratio, the following equation was used:

$$w = M_{NIPAM}m_{NIPAM} + M_{MBA}m_{MBA} + M_{AA}m_{AA}$$

where w is the weight of the dry polymer determined gravimetrically, and M and m are molar mass and moles of the monomer, respectively. The contribution of the initiator to the weight of the polymer is deemed negligible. This equation may be rearranged to obtain the molar ratio of AA to NIPAM.

$$\frac{m_{AA}}{m_{NIPAM}} = \frac{M_{NIPAM} + M_{MBA} \left(\frac{m_{MBA}}{m_{NIPAM}} \right)}{\frac{w}{m_{AA}} - M_{AA}}$$

m_{AA} was determined through potentiometric titration and it was assumed that all MBA added was polymerized (hence, $\frac{m_{MBA}}{m_{NIPAM}} = 0.10$). In our synthesis, $w = 0.06 \text{ g}$ and $m_{AA} = 3.64 \times 10^{-5} \text{ moles}$, so that the molar ratio of AA to NIPAM equaled 0.08.

To determine the molar ratio of tetradecylamine to NIPAM from the ¹³C NMR spectrum, peak A (two NIPAM methyls and a tetradecylamine methylene) and peak 4 (nine tetradecylamine methylenes) were integrated and normalized to peak A. Hence, the following two equations apply:

$$\begin{aligned} \text{Integral of peak A:} \quad m_{C14} + 2 m_{NIPAM} &= 1 \\ \text{Integral of peak 4:} \quad 9 m_{C14} &= 0.34 \end{aligned}$$

where m_{C14} is the moles of tetradecylamine. Solving the equations yielded a molar ratio of tetradecylamine to NIPAM ($\frac{m_{C14}}{m_{NIPAM}}$) of 0.079. Since, $\frac{m_{C14}}{m_{NIPAM}} \approx \frac{m_{AA}}{m_{NIPAM}}$, it was deemed that essentially 100% of the AA were hydrophobically modified.

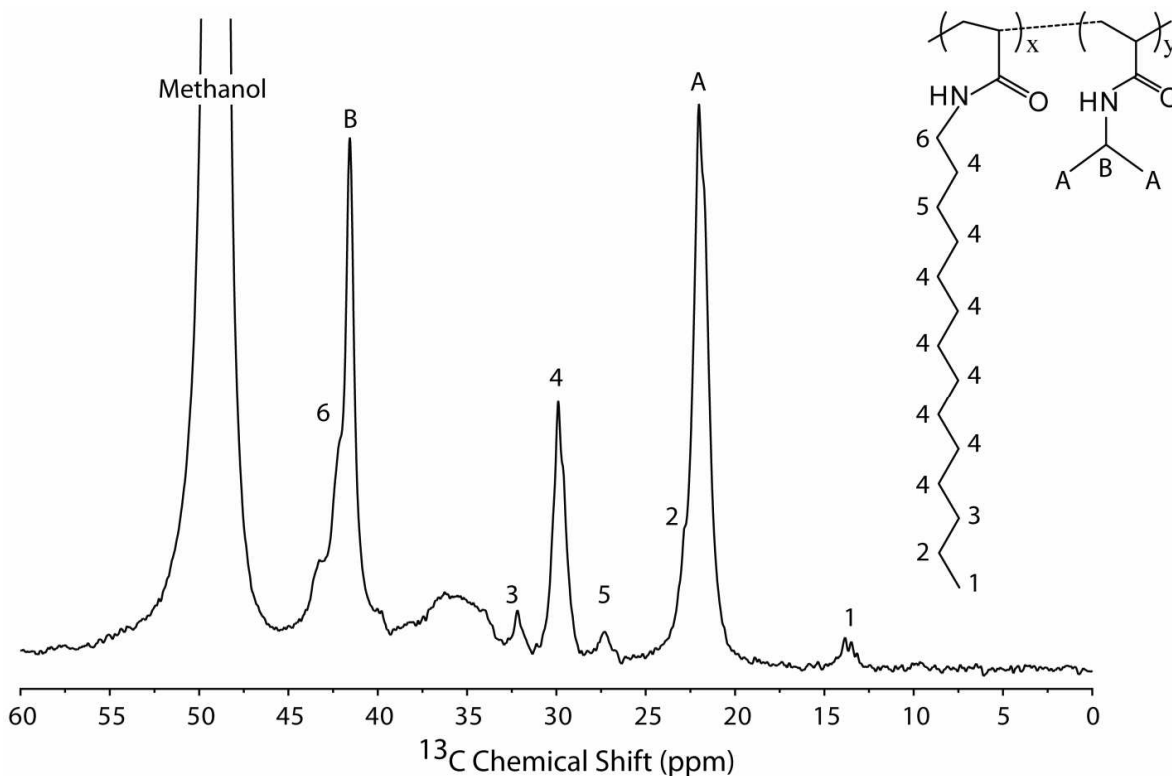


Figure S1: ^{13}C NMR spectrum of HM microgels in methanol. Only the pNIPAM methyls (A) and methyne (B) and the tetradecylamide methylenes (2-6) and the methyl (1) are assigned. The two NIPAM methyls (A) and the nine hydrophobe methylenes (4) are well separated and so, their integrals provide a ready means to determine the extent of hydrophobe incorporation. The carbonyl region of the spectrum is not shown.

Fluorescence Recovery After Photobleaching (FRAP) Simulation:

The FRAP experiment on a Lipogel was simulated with a custom program written in LabView 8.2 (National instruments). The program accepts multiple input parameters describing all aspects of the Lipogel and our microscope setup. These include: Lipogel radius, number of fluorophores, diffusion coefficients, excitation wavelength, pinhole size, photobleaching position, photobleaching intensity, probing time step, observation window, imaging area size and resolution. A snapshot of the simulation program is shown in Figure S2.

Typically, the simulations modeled a scenario in which 50,000 fluorophores were uniformly distributed on the surface of a sphere of 650 nm radius. All fluorophores were assumed to have identical extinction coefficients and molecular brightness. The photobleaching probability depends exclusively on the excitation profile of the laser beam: $1 - c \times f(x, y, z)$, where c is a constant depending on the photobleaching intensity and $f(x, y, z)$ is the Gaussian approximation of the excitation profile¹. A random number between 0 and 1 is generated for each fluorophore on the surface: if the random number is larger than the estimated photobleaching probability, the fluorophore is photobleached and will be invisible in the recovery simulations. The constant c was chosen to closely match the simulated image immediately after the photobleaching pulse to its experimental counterpart (Figure 4B).

The diffusion of the fluorophores was implemented using a Monte Carlo simulation of a 2-D random walk on the surface of the sphere. The step size of random walk was as assumed constant, $\sqrt{4D\tau}$, where D and τ are the user-selected diffusion constant and the sampling time step. The next position of each fluorophore was generated by selecting an arbitrary point on the circle of radius $\sqrt{4D\tau}$ around the current position on the on surface of the sphere. For each fluorophore, the contribution to the detected fluorescence signal is proportional to the apparent detection efficiency $CEF(x, y, z)$ of the objective, which depends on fluorophore position, pinhole size and beam waist¹. Each time step, after all fluorophores move to a new position, the fluorescence signal is obtained by summing up all their $CEF(x, y, z)$ values. Finally, the FRAP curve was normalized to the estimated signal before photobleaching and it was fitted with a biexponential model $Y = B - A_1 e^{-t/\tau_1} - A_2 e^{-t/\tau_2}$ in Origin 7.0 (OriginLab Cooperation). Best fit was found when reduced chi-square converged.

At first, FRAP simulations were run assuming only one diffusing component. As shown in Figure S3, this gives rise to a monoexponential recovery, in stark disagreement with the biphasic behavior observed in experiments (Figure 4 D). However, the single-component diffusing model was used to determine the diffusion constants that closely match the

two recovering times found by fitting the experimental curve (Table 2). These values were then used to simulate the two-component model, with their fractions chosen to find the best match with the experimental FRAP curve (Figure 4E).

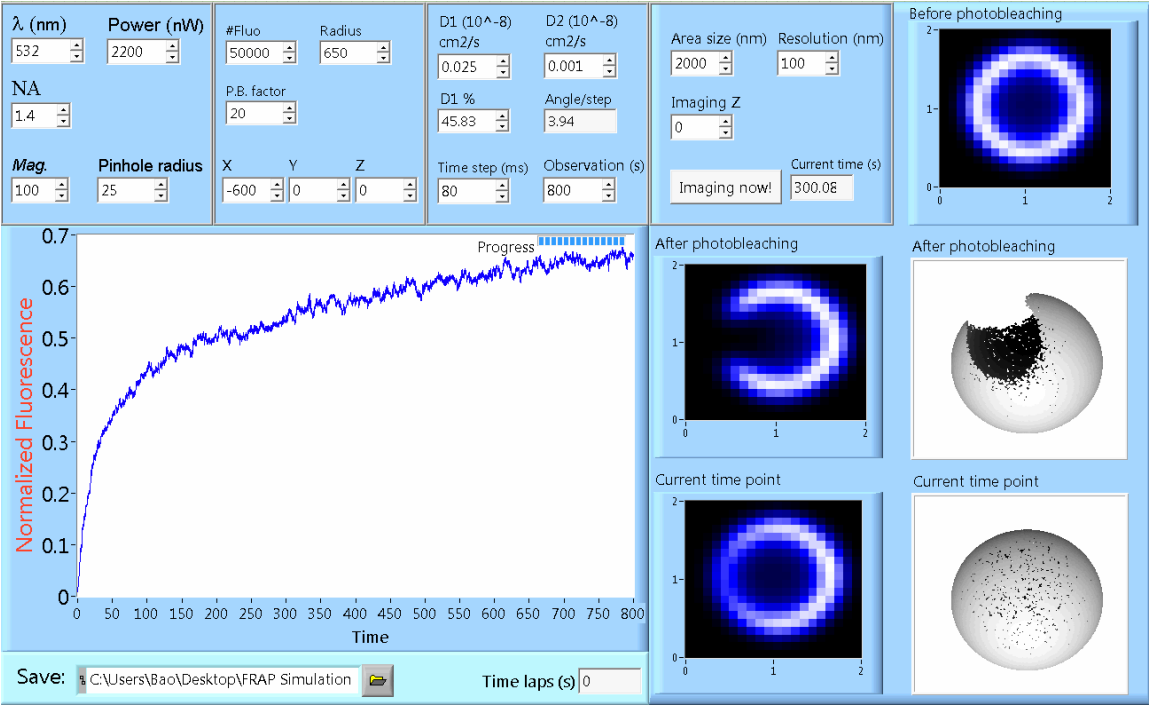


Figure S2: FRAP simulation for a uniformly labelled sphere. The computed recovery curve is shown, together with three simulated images: before, immediately after and 5 min. after instant photobleaching. The 3D plots show the non-bleached fluorophore distribution immediately after photobleaching and after a 5 min. delay.

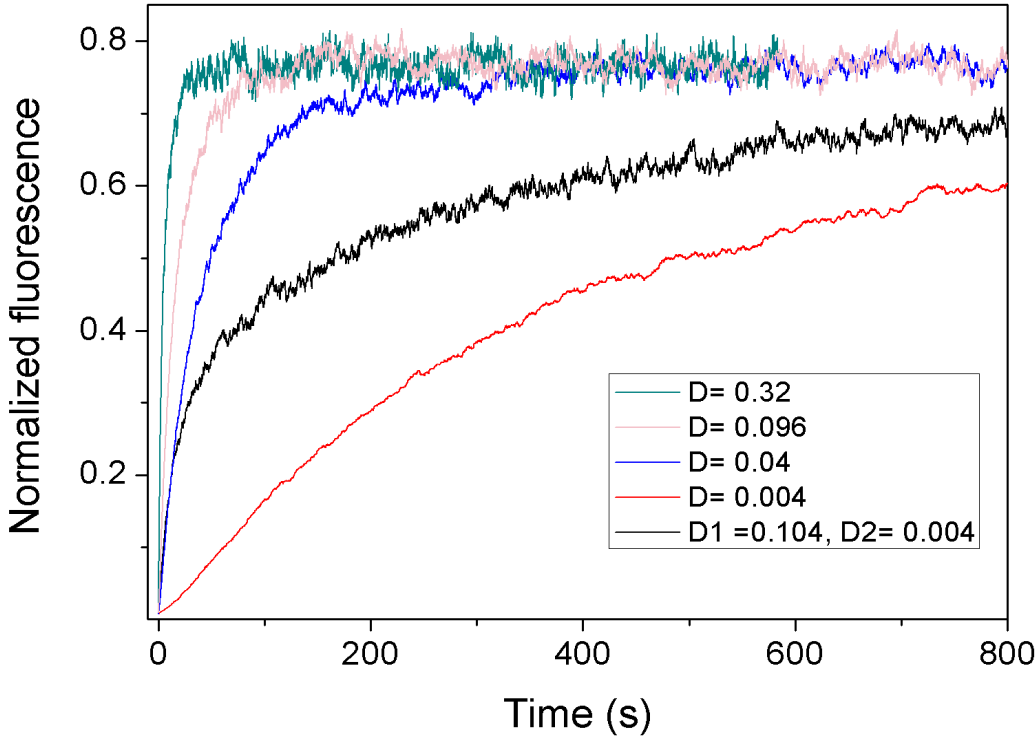


Figure S3: Simulated FRAP curves using one-component model (green, magenta, blue and red) and two-component model (black). The diffusion constants for each curve are given in units of $10^{-8} \text{ cm}^2/\text{s}$.

References:

(1) Wohland, T. *Biophys. J.* **2001**, *80*, 2987-2999.